

WAVELET ANALYSIS OF INCLUSIVE ${}^4\text{He}(e,e')$ SPECTRUM AND MISSING ENERGY SPECTRUM IN REACTION ${}^{12}\text{C}(\gamma,p){}^{11}\text{B}$

A.S. Omelaenko

National Science Center "Kharkov Institute of Physics and Technology", Kharkov, Ukraine

We demonstrated that the standard contour plot of the wavelet transform with wavelet "Mexican Hat" of the inclusive ${}^4\text{He}(e,e')$ spectrum and missing energy spectrum in reaction ${}^{12}\text{C}(\gamma,p){}^{11}\text{B}$ does not give reliable visual indication of the maxima in experimental spectra. We used the scale disconvolution of the initial spectra to construct more informative image in the energy-scale plane.

PACS: 13.75Gx

1. INTRODUCTION

It is just twenty years ago term "wavelet" was introduced into the scientific usage [1]. For this time wavelet analysis (WA) become a powerful common tool for a many investigations in the fields of applied sciences, physics and mathematics. A theoretical treatment of the wavelet analysis is developed in several monographs beginning from [2]. In Russian the substantial review article of the basic theory of the wavelet analysis appeared in 1996 [3]. A useful guide for application of the discrete wavelet transform in computational practice is presented in [4]. The recent article [5] contains the concise digest of the continuous version of the WT and its applications to the e^+e^- annihilation into hadron states with quantum numbers of ρ and ω mesons, and to the p -wave $\pi\pi$ scattering.

The objective of our investigation is to assess the use wavelet analysis for nuclear reactions. For this assessment we choose spectrum of inclusive scattering of the high-energy electrons on ${}^4\text{He}$ nuclei [6] and missing energy spectrum in the typical low energy nuclear reaction ${}^{12}\text{C}(\gamma,p){}^{11}\text{B}$ taken from work [7]. We used the so-called wavelet "Mexican Hat" considered as the most suitable due to its good localization and small number of oscillations. In particular we have demonstrated that at least for two examples at consideration the visual inspection of the standard wavelet transformation (WT) of a one-dimension initial spectrum (diffuse two-dimension energy-scale image) practically couldn't give a reasonable idea about the position of the maxima in the original spectrum. Trying to shed some light on this unexpected circumstance it is relevant to remember that WT is defined as projection of initial spectrum on the wavelet with scale a at position b . Of course, such a value depends on the characteristic details of a spectrum being at the same time sensitive to the strong energy dependence of the wavelet used. To relax influence of the latter factor we have considered the contribution of all wavelets with scale a (that is integrated of on their position) to the point t of initial spectrum as a function to plot the energy-scale image (scale unfolded spectrum). The energy-scale image of such an averaged value exhibits all characteristic features of a complicated nuclear reaction spectrum.

2. WAVELET TRANSFORMATION AND RECONSTRUCTION

The underlying notion of the wavelet theory with continuous variables is a biparametric family of self-similar soliton-like functions generated by dilatation (the scale parameter a) and translation (the parameter b) of some analyzing function $\psi(t)$ (by tradition the variable t is called “time” even in the case of energy or some other variable):

$$\psi_{a,b}(t) = |a|^{-1/2} \psi\left(\frac{t-b}{a}\right). \quad (1)$$

The main points of the wavelet theory is formula for WT being a convolution of initial function $f(t)$ with wavelet ψ :

$$w(a,t) = C_{\psi}^{-1/2} |a|^{-1/2} \int_{-\infty}^{\infty} \psi\left(\frac{t'-t}{a}\right) f(t') dt' \quad (2)$$

and the inverse transformation (reconstruction of the function $f(t)$):

$$f(t) = C_{\psi}^{-1/2} \int_{-\infty}^{\infty} \int_{-\infty}^{\infty} \psi\left(\frac{t-t'}{a}\right) w(a,t') \frac{dt' da}{|a|^{5/2}}. \quad (3)$$

The normalizing constant C_{ψ} can be presented as the following integral on variable ω :

$$C_{\psi} = \int_{-\infty}^{\infty} |\psi(\omega)|^2 |\omega|^{-1} d\omega, \quad (4)$$

involving the Fourier transformation of the wavelet used:

$$\psi(\omega) = \int_{-\infty}^{\infty} \psi(t) e^{i\omega t} dt. \quad (5)$$

The graphic representation of the $w(a,t)$ as contour plots in scale-time plate is used in WA as significant tool for visual resolving the structures in the initial spectrum. Besides, implementation of some restrictions at integration on time and scale variable give broad lands for processing of data by separation of the scale band contributions, noise filtering and so on.

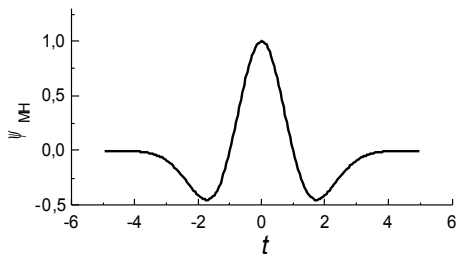
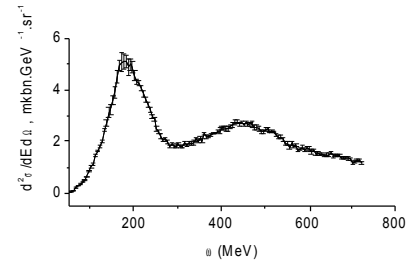
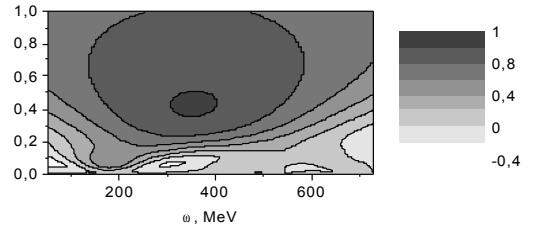


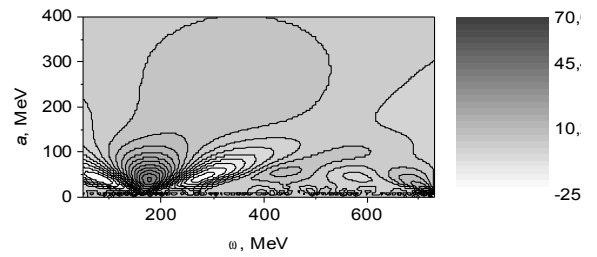
Fig. 1. Wavelet “Mexican Hat”



a)



b)



c)

Fig. 2. The spectrum of inclusive 1269 MeV scattering from ^4He nucleus at angle 30° ([5]), a), its wavelet transform and the scale unfolded spectrum (c)

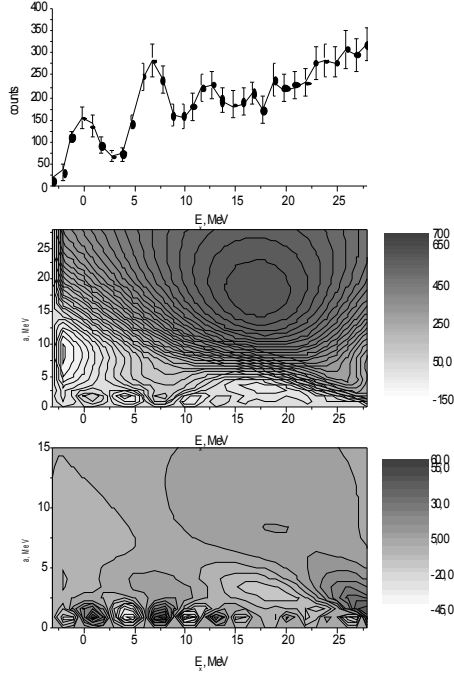


Fig. 3. Missing mass spectrum for reaction $^{12}\text{C}(\gamma, p)^{11}\text{B}$ from work [6] (a), its wavelet transform (b) and scale unfolded spectrum (c)

3. SCALE UNFOLDED SPECTRUM (SUS)

To get some different approach to building of a scale-energy image we have changed order of integration in Eq. (3) and have written down the spectrum reconstructed through the lens of the wavelet analysis in form of a convolution on the scale a :

$$f(t) = \int_{-\infty}^{\infty} f(a, t) da. \quad (6)$$

In Eq. (6) $f(a, t)$ is a contribution to the initial spectrum per scale unit at current a (scale unfolded spectrum):

$$f(a, t) = \int_{-\infty}^{\infty} f(t') \delta_{\psi} \left(\frac{t-t'}{a} \right) dt' \quad (7)$$

with the function

$$\delta_{\psi} \left(\frac{t-t'}{a} \right) = \frac{\text{sign } a}{C_{\psi} a^3} \int_{-\infty}^{\infty} \psi \left(\frac{t-t''}{a} \right) \psi^* \left(\frac{t'-t''}{a} \right) dt''. \quad (8)$$

In Eqs. (7,8) the argument of δ_{ψ} is written in fashion characteristic for a wavelet function (Eq. (1)). Indeed, such a specification is manifested by the next formula:

$$\delta_{\psi} \left(\frac{t-t'}{a} \right) = \frac{1}{2\pi a^2 C_{\psi}} \int_{-\infty}^{\infty} |\hat{\psi}(\omega)|^2 \exp \left(i\omega \frac{t-t'}{a} \right) d\omega. \quad (9)$$

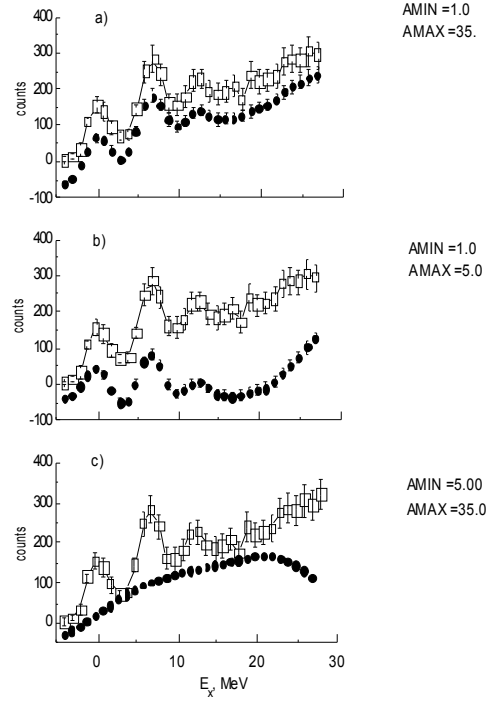


Fig. 4. Missing mass spectrum for reaction $^{12}\text{C}(\gamma, p)^{11}\text{B}$ from work [6] (black squares with line) and the same spectrum after reconstruction within scale bands $a_{\min}=1, a_{\max}=35$ (a); $a_{\min}=1, a_{\max}=5$ (b); $a_{\min}=5, a_{\max}=35$ (c); all shifted downwards to avoid confusion with initial spectrum

It is interesting to note that independently of the wavelet used integrating of this function on scale parameter a yields the Dirac δ function:

$$\int_{-\infty}^{\infty} \delta_{\psi} \left(\frac{t-t'}{a} \right) da = \delta(t-t'). \quad (10)$$

So, Eq. (10) signifies that the function $\delta_{\psi}((t-t')/a)$ can be treated as a result of the scale unfolding of the δ function itself on the base of wavelet ψ . Further, from the fact that the wavelets are introduced as functions an average values of which are equal to zero it follows

$$\int_{-\infty}^{\infty} \delta_{\psi} \left(\frac{t-t'}{a} \right) dt = \int_{-\infty}^{\infty} \delta_{\psi} \left(\frac{t-t'}{a} \right) dt' = 0. \quad (11)$$

Similar to the standard WT the function defined by Eq. (7) can be depicted as contour plot in scale-time plane. But it should be stressed that the time arguments for the both functions have the quite different meaning. In the case of WT one has to do with the coordinate of the projection of an initial signal on the wavelet with his inherent strong time dependence. It is necessary integration on time to get contribution to the initial spectrum at parameter a (Eq. (3)). On the contrary, our function $f(a, t)$ represents direct contribution to the t point of the spectrum due to all wavelets with fixed scale value a irrespective of their localization. For $f(a, t)$ influence of the energy dependence of the wavelet used

is smoothed over with holding good of scale dependence being the distinguishing feature of the wavelet conception. So, one can anticipate that the contour image of the $f(a,t)$ would give more robust reflection of the specific details of the initial spectrum.

4. WT AND SUS: NUMERICAL COMPARISON

In this communication we have restricted our self by calculations with the wavelet “Mexican Hat” (MH, Fig. 1):

$$\psi_{MH}(t) = (1 - t^2)\exp(-t^2/2). \quad (12)$$

For MH $C_\psi = C_{MH} = 2\pi$ and Eq. (8) turns into

$$\delta_{MH}\left(\frac{t-t'}{a}\right) = \frac{1}{32\sqrt{\pi}a^2} \times \left[\left(\left(\frac{t-t'}{a} \right)^2 - 6 \right)^2 - 24 \right] \exp\left(-\frac{1}{4}\left(\frac{t-t'}{a}\right)^2\right). \quad (13)$$

The wavelet transformation images the inclusive electron scattering spectrum from ${}^4\text{He}$ [5] (Fig. 2, a) and the missing energy spectrum for ${}^{12}\text{C}(\gamma,p){}^{11}\text{B}$ [6] (Fig. 3, a) are shown on panels b) of Figs. 3,4. In calculations the initial spectra were presented by broken lines coming through the neighboring experimental points $f_k \equiv f(t_k)$. That is $f(t) = f(t; f_1, \dots, f_k, \dots, f_n)$, n being the number of points.

For inclusive spectrum the most characteristic feature presented by the contour WT plot in the energy-scale plate is the wide overall maxima at $\omega \sim 350$ MeV and $a \sim 400$ MeV. From low scales corresponding “hill” adjoins to the narrow gully. This gully ensures appearance of two well known from the physical point of view maxima at reconstruction of the initial experimental spectrum: the large quasi-elastic peak and the lower one corresponding to the excitation of the first nucleon resonance.

On the other hand, the quasi-elastic peak and the resonance peak are displayed immediately by the image of the scale unfolded inclusive spectrum (Fig. 2,b) as clearly seen hills. Minimum between them corresponds to so-called “dip” region of the spectrum. The SUS image allows also distinguishing on the left hand side of quasi-elastic peak some manifestation of an additional dip region. The white spots of the dip-regions have a specific elongated form and are symmetric orientation relatively to the quasi-elastic peak. There are seen the numerous small-scale structures due to the noise-like high-frequency contributions. The structure at the right side of the SUS image can be treated as excitation of the Roper resonance being obscured by experimental problems at the end of the measured spectrum.

For the missing energy spectrum from work [7] comparison of the standard WT image (Fig. 3,b) and our SUS image (Fig. 3,c) is not so contrasting as in the case of the inclusive scattering. Nevertheless, one can make certain that on the SUS image the location of the on the missing mass spectrum for reaction ${}^{12}\text{C}(\gamma,p){}^{11}\text{B}$ (Fig. 4a), reconstruction within the scale bands containing the characteristic resonance structures

(Fig. 4b) and contribution of large-scale background (Fig. 4c). For this goal we have used coming from Eqs.(6,7) formula with relevant limits a_{\min} , a_{\max} at integration on scale and with integration on energy in limits of the experimental spectra:

$$f(E) = \iint f(E') \delta_{MH}(a, E, E') dE' da. \quad (14)$$

Errors were calculated according to

$$\delta_i^2 = \sum_k \left(\delta_k \iint \frac{\partial f(E'; f_1, \dots, f_k, \dots, f_n)}{\partial f_k} \delta_\psi \left(\frac{E-E'}{a} \right) dE' da \right)^2$$

with summing on the experimental points.

5. DISCUSSION

The numerical calculations that we describe in this paper show that for complicated nuclear spectra with overlapping resonances the standard WT contour scale-time images are not a robust tool of visual indication with respect to the properties of the initial signal. Indeed, the WT image reflects characteristic feathers of both the initial signal and the wavelet used in analysis and influence of the latter may surpass the role of the small resonance structures. It should be kept in mind that experimental spectra are of restricted length.

The main result of this paper is the suggestion to use the SUS image that is free from this shortage. Using SUS images demonstrates some additional potentialities of the WA.

Reconstruction of the original function in the framework of the wavelet analysis involves integration on two time variables and the scale. Because in applications one is dealing with finite-length time intervals instead of $(-\infty \dots +\infty)$ used in the theory there will appear some errors at integration on time (this effect is known as “cone of influence” [8]). From Eqs.(1,2) it follows that coming from WT standard reconstruction involves two such approximate time integrations. Some advantage of our approach is that one of time integrations for given wavelet is taken analytically in theoretical infinity limits at calculation of the $\delta_\psi(a,t,t')$. It is interesting to note that the latter is the scale-unfolding of the Dirac δ function.

REFERENCES

1. A. Grossman, J. Morlet. Decomposition of Hardy functions into square integrable wavelets of constant shape // *SIAM J. Math. Anal.* 1984, v. 15, p. 723-736.
2. I. Daubechies. *Ten lectures on wavelets*. Society for industrial and applied mathematics. 1992, 357 p.
3. N.M. Astaf'eva. Wavelet analysis: basic theory and some applications // *Uspehi Fiz. Nauk.* 1996, v. 166, p. 1145-1170 (in Russian).
4. I.M. Dremin, O.V. Ivanov, V.A. Nechitailo. Wavelets and their applications // *Uspekhi Fiz. Nauk.* 1996, v. 171, p. 465-501 (in Russian).
5. T.S. Belozerova, P.G. Frick, V.K. Henner. Wavelet analysis of data in particle physics: vector mesons in

- e^+e^- annihilation // *Yad. Fiz.* 2003, v. 66, p. 1269-1281.
6. E.L. Kuplennikov et al. Examination of the cross sections ${}^4\text{He}(e,e')$ reaction in the quasifree, dip and Δ (1232)-resonance region // *Yad. Fiz.* 1994, v. 57, p. 771-776.
 7. P.D. Hartry et al. ${}^{12}\text{C}(\gamma,p){}^{11}\text{B}$ cross section from 80 to 157 MeV // *Phys. Rev. C*, 1995, v. 51, p. 1982-1990.
 8. Ch. Torrence and G.P. Compo. A practical guide to wavelet analysis // *Bull. Amer. Met. Society*. 1998, v. 79, p. 61-78.

ВЕЙВЛЕТ-АНАЛИЗ ИНКЛЮЗИВНОГО ${}^4\text{He}(e,e')$ -СПЕКТРА И СПЕКТРА ПОТЕРЯННОЙ ЭНЕРГИИ В РЕАКЦИИ ${}^{12}\text{C}(\gamma,p){}^{11}\text{B}$

А.С. Омелаенко

Показано, что стандартные контурные графики вейвлет-трансформа с вейвлетом “Мексиканская шляпа” инклюзивного ${}^4\text{He}(e,e')$ -спектра и спектра потерянной энергии в реакции ${}^{12}\text{C}(\gamma,p){}^{11}\text{B}$ не обеспечивают надежной визуальной индикации максимумов экспериментальных спектров. Для построения более информативного образа в масштабно-энергетической плоскости использована масштабная развертка исходных спектров.

ВЕЙВЛЕТ-АНАЛИЗ ИНКЛЮЗИВНОГО ${}^4\text{He}(e,e')$ -СПЕКТРА ТА СПЕКТРА ЗАГУБЛЕНОЇ ЕНЕРГІЇ В РЕАКЦІЇ ${}^{12}\text{C}(\gamma,p){}^{11}\text{B}$

О.С. Омелаєнко

Показано, що стандартні контурні графіки вейвлет-трансформа з вейвлетом “Мексиканська шляпа” інклюзивного ${}^4\text{He}(e,e')$ -спектра і спектра загубленої енергії в реакції ${}^{12}\text{C}(\gamma,p){}^{11}\text{B}$ не забезпечують надійної візуальної індикації максимумів експериментальних спектрів. Для побудови більш інформативного образу в масштабно-енергетичній площині використано масштабну розгортку початкових спектрів.